

Development of an advanced A-TIG (AA-TIG) welding method by control of Marangoni convection

Hidetoshi Fujii^{a,*}, Toyoyuki Sato^b, Shanping Lu^{a,c}, Kiyoshi Nogi^a

^a *Joining and Welding Research Institute, Osaka University, Osaka 567-0047, Japan*

^b *Welding Technology Center, Taiyo Nippon Sanso Corporation, Yamanashi 408-0015, Japan*

^c *Institute of Metal Research Institute, Chinese Academy of Science, Shenyang 110016, PR China*

Received 20 June 2007; received in revised form 13 October 2007; accepted 17 October 2007

Abstract

A new type of tungsten inert gas (TIG) welding has been developed, in which an ultra-deep penetration is obtained. In order to control the Marangoni convection induced by the surface tension gradient on the molten pool, He gas containing a small amount of oxidizing gas was used. The effect of the concentration of O₂ and CO₂ in the shielding gas on the weld shape was studied for the bead-on-plate TIG welding of SUS304 stainless under He–O₂ and He–CO₂ mixed shielding gases. Because oxygen is a surface active element for stainless steel, the addition of oxygen to the molten pool can control the Marangoni convection from the outward to inward direction on the liquid pool surface. When the oxygen content in the liquid pool is over a critical value, around 70 ppm, the weld shape suddenly changes from a wide shallow shape to a deep narrow shape due to the change in the direction of the Marangoni convection. Also, for He-based shielding gas, a high welding current will strengthen both the inward Marangoni convection on the pool surface and the inward electromagnetic convection in the liquid pool. Accordingly, at a welding speed of 0.75 mm/s, the welding current of 160 A and the electrode gap of 1 mm under the He–0.4%O₂ shielding, the depth/width ratio reaches 1.8, which is much larger for Ar–O₂ shielding gas (0.7). The effects of the welding parameters, such as welding speed and welding current were also systematically investigated. In addition, a double shielding gas method has been developed to prevent any consumption of the tungsten electrode.

© 2008 Elsevier B.V. All rights reserved.

Keywords: Weld shape; Oxygen; Helium; Marangoni convection; Electromagnetic convection; Double shielding gas

1. Introduction

Tungsten inert gas (TIG) welding is one of the most popular welding processes in various manufacturing industries due to the obtained good weld bead surface and a very high quality weld metal without any weld defects. However, compared to other arc welding processes, such as gas metal arc welding, plasma arc welding, or submerged arc welding, the shallow penetration of the TIG welding restricts its ability to weld thick structures in a single pass, thus its productivity is relatively low. Therefore, in order to increase the TIG welding production, the demand for control of the weld shape with a deep penetration is steadily increasing, and has been a concern for a long time.

Recently, a novel modification of the TIG process, namely, active flux TIG (A-TIG), which was first proposed by the E.O. Paton Institute of Electric Welding in the 1960s [1], has been brought to many researchers' attention since the 1980s. Even though some fluxes for the A-TIG process are commercially available and have been used in industry, there is still no common agreement on the understanding of the A-TIG mechanism. Four main physical mechanisms have been proposed. The first is that a lowering of the surface tension of the molten pool by the flux results in an increased depression of the surface of the weld pool to provide an increased radius of curvature of the weld pool surface to support the arc pressure, which is also called the TIG keyhole mode [2]. The second mechanism is the arc constriction produced by the vaporized flux molecules [3–10]. The third one is the reversal of the Marangoni convection, which is induced by the change in the sign of the temperature coefficient of the surface tension when the surface active element is over the critical value in the liquid pool [11–17]. Recently, Lowke

* Corresponding author. Tel.: +81 6 6879 8653; fax: +81 6 6879 8653.
E-mail address: fujii@jwr.osaka-u.ac.jp (H. Fujii).

and co-workers proposed another mechanism call the insulation mode [18].

The authors performed systematic experiments by controlling the amount of oxides for many kinds oxides as the active fluxes, and concluded that almost all kinds of oxides, instead of only TiO₂ and SiO₂, can be the active flux, and the reversal of the Marangoni convection in the weld pool with different surface active elements is the main mechanism for the A-TIG welding [16,17]. There is an effective range for the deep penetration, because the temperature coefficient of the surface tension is positive only when the oxygen content in the molten pool is between 70 ppm and 300 ppm [16,17]. Furthermore, based on the obtained experimental results, the authors discovered that even the small addition of an active gas, such as O₂ and CO₂, to the inert argon-base shielding gas instead of the oxide flux on the plate can significantly increase the weld penetration [19–21]. Compared to the A-TIG welding, the mixed shielding gas is easily controlled and can be applied by automatic industrial TIG welding equipment. The effective ranges for the O₂ and CO₂ concentrations in the shielding gas are the same because of the significant dissociation reactions of O₂ and CO₂ in the high temperature arc plasma column [19].

Helium is another important inert gas for TIG welding. Compared to argon, its current density at the anode spot on the liquid pool under He shielding is high, which will directly increase the electromagnetic force and possibly increase the temperature gradient on the pool surface. Since the strength of the Marangoni convection is controlled by the combination of the temperature gradient on the pool surface and the temperature coefficient of the surface tension, the helium should have a more significant effect on the Marangoni convection. In this study, He–O₂ and He–CO₂ shielding gases were selected to investigate the effect of the shielding gas concentration and welding variables on the oxygen adsorption by the liquid pool, Marangoni convection and the final TIG weld shape.

The shielding gas containing a small amount of oxidizing gas might cause an acceleration of the electrode consumption. Unless the welding time is very short like a spot welding, this

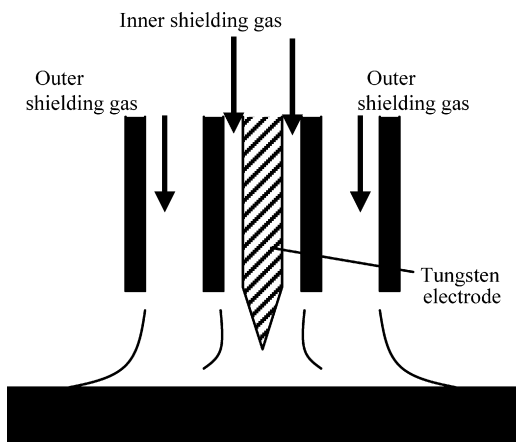


Fig. 1. Schematic diagram of double shielding torch for GTA welding.

Shielding gas	Weld shape
Pure He	
He-0.4%CO ₂	
He-4.0%CO ₂	

Fig. 2. Weld shapes under different He–O₂ mixed shielding gases (160 A, 2 mm/s, 3 mm arc length).

matter cannot be disregarded. Accordingly, we developed a new TIG welding process with a significantly deep penetration without any consumption of the tungsten electrode by using a double shielding torch.

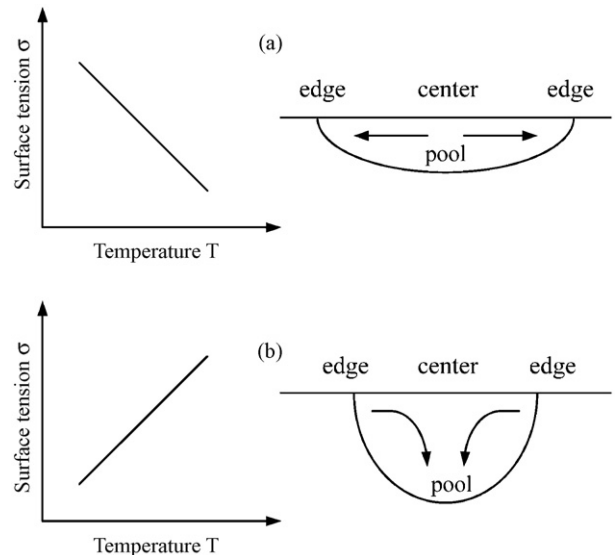


Fig. 3. Marangoni convection mode in the weld pool: (a) $\partial\sigma/\partial T < 0$; (b) $\partial\sigma/\partial T > 0$.

2. Experimental procedure

The experimental welding is bead-on-plate using SUS304 stainless steel plates (100 mm × 50 mm × 10 mm) with a lower sulfur content of less than 20 ppm in a flat position without supplying filler metals. A direct current, electrode negative (DCEN) polarity power source (YC-300BZ1) was used with a mechanized system in which the test piece was moved at a constant speed. A water-cooled normal torch with a thoriated tungsten electrode (W-2%ThO₂, 2.4 mm diameter) was used in the experiments. The vertex angle of the electrode was 60°.

For the first experiments, all the bead-on-plate welds were made at the welding current of 160 A, welding speed of 2 mm/s and 3 mm electrode gap, except that the torch gas concentration was varied between pure helium and helium with 4%O₂. The effects of the welding parameters including the welding current and welding speed on the weld shape were then separately investigated under pure He and He-0.4%O₂ shielding. The welding current was varied from 80 A to 250 A, and the welding speed was changed between 0.75 mm/s and 5.0 mm/s.

For the next step, a double shielding torch was used to decrease the consumption of the tungsten electrode. A schematic diagram of the double shielding torch is shown in Fig. 1. The

outer shielding gas was a He-O₂ or He-CO₂ mixed gas, and the inner shielding gas was pure He gas.

After welding, all the weld beads were sectioned and the specimens for the weld shape observations were prepared by etching using a HCl + Cu₂SO₄ solution to reveal the bead shape and dimensions. The cross-sections of the weld beads were photographed using an optical microscope (Olympus HC300 Z/OL). The oxygen content in the weld metal was analyzed using an oxygen/nitrogen analyzer (Horiba, EMGA-520). Samples for the oxygen measurements were cut directly from the weld metal.

Some test plates (500 mm × 300 mm × 10 mm) were welded with I type butt joints by a one pass layer from both the face and the back side using the double shielding torch. The mechanical properties of the welded joints were evaluated using a tensile test, a bending test, and a V-notched Sharpy impact test.

3. Results and discussion

3.1. Weld shape and Marangoni convection

Typical weld cross-sections are shown in Fig. 2 for the different torch gas shielding conditions from pure He to He-4%O₂ shielding at the welding current of 160 A, welding speed of

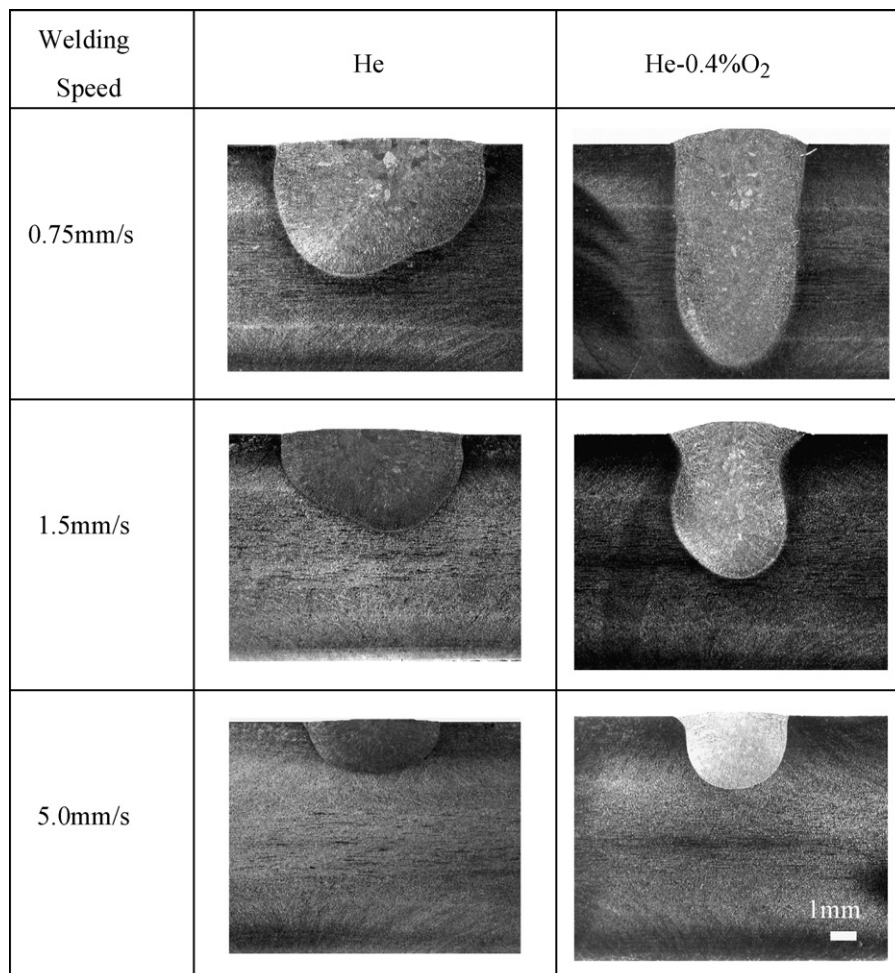


Fig. 4. Weld shapes at different welding speeds for pure He and He-0.4%O₂ shielding gases.

2 mm/s and the electrode gap of 3 mm. Under pure He and He–0.1%O₂ shielding, relatively wide and shallow welds were produced. When the oxygen content in the shielding gas is in the range of 0.2–2.0%, the weld shape become relatively narrow and deep. With a further increase in the oxygen content of the shielding gas, it is interesting to find that the weld shape becomes shallow and wide again. These results are quite similar to the results for the Ar–O₂ or Ar–CO₂ shielding gas, except that the penetration depth is greater for the He–O₂ shielding gas.

The weld depth/width (D/W) ratio is lower at around 0.4 under pure He shielding and He–0.1%O₂ mixed shielding, and abruptly increases and reaches 0.6 when the oxygen concentration in the shielding gas is between 0.2% and 2.0%. This sharp increase in the D/W ratio indicates that the fluid flow pattern in the liquid pool is changed, as shown in Fig. 3. When the torch gas oxygen concentration is over 2%, the weld D/W ratio decreases again.

The weld shape depends to a large extent on the different fluid flow modes in the welding pool, and the Marangoni convection induced by the surface tension on the pool surface is the main convection that significantly influences the fluid flow in the liquid pool [12,22–24]. Generally, the surface tension σ decreases with the increasing temperature T , $\partial\sigma/\partial T < 0$, for a pure metal and many alloys. Since there is a large temperature gradient existing on the welding pool surface between the center under the torch and the edges of the weld pool, a large surface tension gradient will be produced along the surface. In the weld pool for such materials, the surface tension is higher in the cooler part of the pool, i.e., at the edge, than that in the pool center, under

the arc, and hence, the Marangoni convection flows from the pool center to the edge. The heat flux from the arc power in the pool center is easily transferred to the edge and the weld shape is relatively wide and shallow as shown in Fig. 3(a).

Taimatsu et al. [25] measured the surface tension of the Fe–O system at high temperature and found that the temperature coefficient of the surface tension can change from a negative value to positive when the oxygen content in the Fe–O system is in the range of 150–350 ppm. Sahoo et al. [23] calculated the temperature coefficient of the surface tension for the Fe–O and Fe–S systems and they obtained similar results. The weld metal oxygen content increases with the torch gas oxygen content. Accordingly when the surface active element, such as oxygen and sulfur, exceeds a certain value in stainless steel [11,12], the temperature coefficient of the surface tension ($\partial\sigma/\partial T$) changes from a negative to a positive value, $\partial\sigma/\partial T > 0$, and the direction of the Marangoni convection on the weld pool changes as illustrated in Fig. 3(b). In this case, the heat flux easily transfers from the center to the bottom and a relatively deep and narrow weld is made. The authors' earlier experimental results [16,17] showed that the oxygen was an active element in the SUS304 stainless steel and the temperature coefficient of the surface tension became positive when the oxygen content in the weld pool was in the range of 70–300 ppm.

3.2. Effect of welding conditions on weld shape

Fig. 4 shows the effect of the welding speed on the weld shapes when using a pure He and He–0.4%O₂ mixed shield-

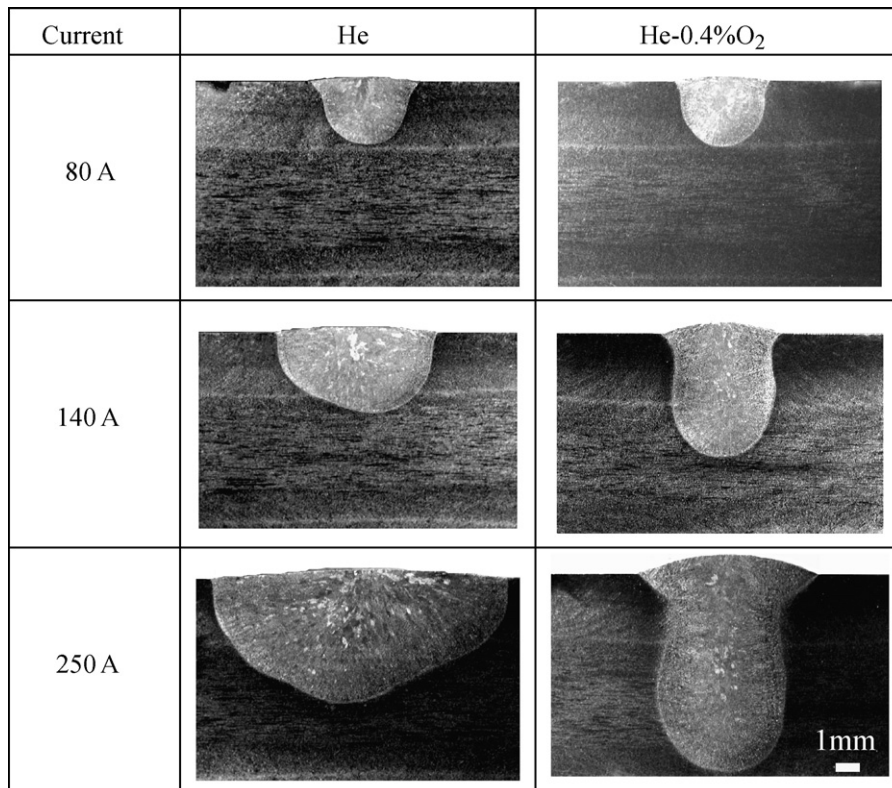


Fig. 5. Weld shapes at different welding currents for pure He and He–0.4%O₂ shielding gases.

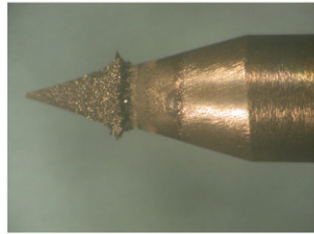
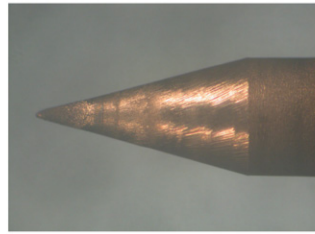

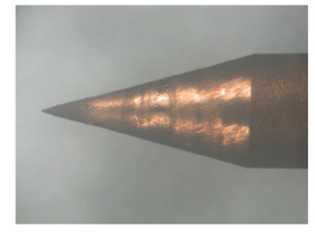
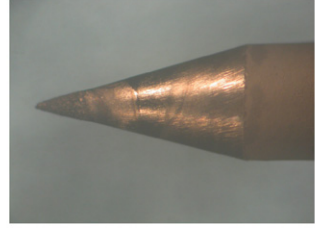
Shielding gas	Normal single torch	Double shielding torch
He-0.2%CO ₂		
He-0.5%CO ₂		
He-1.0%CO ₂	/	
He-5.0%CO ₂	/	
		

Fig. 6. Surfaces of tungsten electrodes after welding by using different shielding torches and shielding gases.

ing gas. The welding speed was varied from 0.75 mm/s to 5.0 mm/s at the constant welding current of 160 A and electrode gap of 1 mm. All the weld shapes are wide and shallow under pure He shielding, and narrow and deep under the He–0.4%O₂

mixed shielding. When the welding speed is 0.75 mm/s with the He–0.4%O₂ shielding, a 9.4 mm weld penetration is obtained for a single pass welding. In this case, the depth/width ratio reaches 1.8, which is much larger for Ar–O₂ shielding gas. The weld

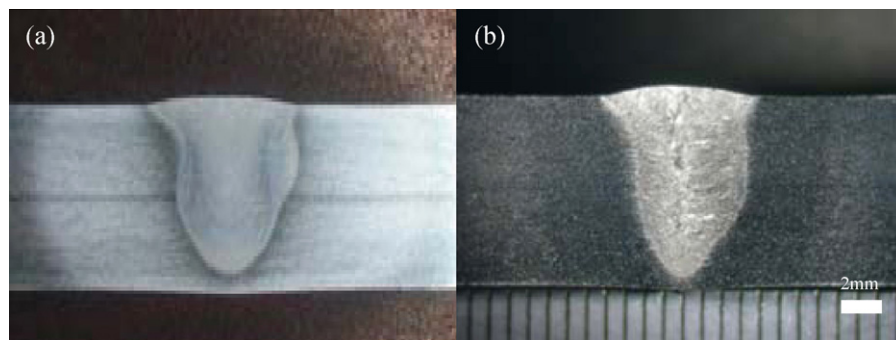


Fig. 7. Comparison of weld shapes between (a) He–O₂ and (b) He–CO₂ as outer shield in double-shielded GTA welding.

metal oxygen content under pure He shielding is around 20 ppm for all conditions and an outward Marangoni convection occurs under pure He, while under a He–0.4%O₂ shielding, the weld metal oxygen content is high between 70 ppm and 110 ppm and an inward Marangoni convection occurs on the liquid pool, thus a deep and narrow weld shape forms.

Fig. 5 shows the effect of the welding current on the weld shape under pure He and He–0.4%O₂ shielding gases. The current was varied from 80 A to 250 A at the constant welding speed of 2 mm/s and electrode gap of 1 mm. The weld shape is relatively wide and shallow under pure He shielding, and narrow and deep under He–0.4%O₂ shielding. Under pure He shielding, the weld *D/W* ratio slightly decreases with the increasing welding current. However, under the He–0.4%O₂ mixed shielding, the weld *D/W* ratio continuously increases with the welding current, which is quite different from the results using Ar–O₂ and Ar–CO₂ mixed shielding gases [20,21], in which the weld *D/W* ratio slightly decreases or maintains a constant value at a welding current higher than 160 A.

Changing the welding current will directly alter the heat input and weld area. The heat distribution of the arc on the weld pool is the main factor affecting the weld shape and weld *D/W* ratio. Tsai and Eagar [26] observed that increasing the welding current would increase the magnitude of the heat intensity, and then the temperature gradient on the pool surface. Therefore, the Marangoni convection on the pool surface should be strengthened with the increasing welding current. Also, the high welding current should increase the strength of the electromagnetic convection in the liquid pool. The numerical study by Tanaka et al. [27] of the GTA welding indicated that the convection flow in the liquid pool was mainly controlled by the Marangoni force and electromagnetic force under pure He shielding. However, under Ar–0.3%O₂ and Ar–0.3%CO₂ shieldings [20,21], the plasma drag force that induces an outward convection in the liquid pool is one of the main convections, and a high welding current will increase the plasma drag force, and thus make the weld *D/W* ratio slightly decrease or maintain a constant value at a high welding current under the Ar–0.3%O₂ or Ar–0.3%CO₂ shielding gas.

3.3. Effect of double shielding torch

A double shielding gas method has been developed to prevent any consumption of the tungsten electrode. Fig. 6 shows the surfaces of the tungsten electrode after welding using the different shielding torches and shielding gas. In this case, the inner gas was pure He and the outer gas was He–CO₂ gas. For the normal torch, a remarkable consumption of the tungsten electrode is clearly observed. On the other hand, for the double shielding torch, there is no consumption of any tungsten electrode even though a substantial amount of oxidizing gas was added.

Fig. 7 shows the effect of the outer shielding gas on the cross-sections of the welds. The inner gas was pure He for both cases and the outer shielding gas was the He–O₂ or He–CO₂ gas. The welding speed, welding current and arc length were 120 A, 1 mm/min and 2 mm, respectively. Fig. 8 shows that the relationship between the oxygen [O] content in the welds and the ratio of the depth to width (*D/W*). It was found that there is no differ-

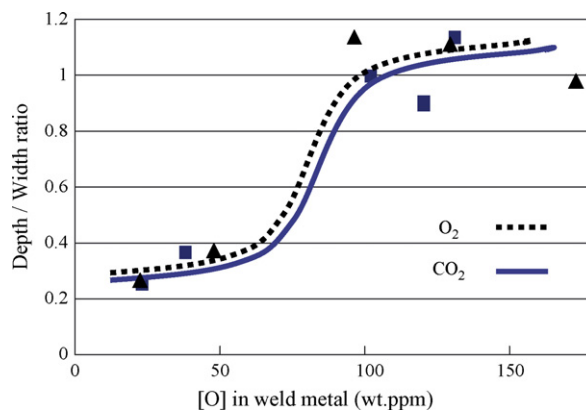


Fig. 8. Relationship between oxygen content in weld pool and depth/width (*D/W*) ratio.

ence in the penetration between the He–O₂ gas and He–CO₂ gas. When the oxygen [O] content of the welds is over 70 ppm, the *D/W* of the welds sharply increases regardless of the oxidizing gas such as O₂ or CO₂, which is completely same as the case for the normal torch.

3.4. Evaluation of the quality of welded joints

Table 1 shows the result of the tensile test for the joints welded under the conditions shown in Section 3.3 using the double shielding gas torch. The tensile strength of the joints is much stronger than the value of the base metal standard (520 N/mm²: JIS G 4304).

Table 2 shows the result of the V-notch Charpy impact test. The test specimens are sub-sized with a three-quarter thickness (7.5 mm), and the test temperature is –196 °C (liquid nitrogen). Both the absorbed energy values of the weld metal and the heat affected zone are sufficient for the TIG welded joint, and the ratio of the ductile fracture area and the lateral expansion also show the high toughness characteristics of this joint.

Fig. 9 shows the bending test results and a photograph of the test specimens after the bending test. The test specimens were bent up to 180° using a guide whose bending radius was twice that of the specimen thickness. There was no defect on either side of all the specimens. These results clearly showed the soundness of the welded joints. Based on these three kinds of mechanical tests, it can be judged that the quality of the welded joints is as good as the normal TIG welding joints, even if these joints are welded using a slightly oxidizing gas as the outer shielding gas.

Therefore, this new welding process using a double shielding torch with a slightly oxidizing gas must be applicable for any important construction made of stainless steel under any severe conditions.

Table 1
Tensile strength of butt joint welded by double-shielded GTA welding

Test specimen no.	Tensile strength (N/mm ²)	Breaking position
T1	593	Weld metal
T2	588	Weld metal

Table 2
Impact test result of butt joint welded by double-shielded GTA welding

Test specimen no.	Position of V-notch	Absorbed energy (J)		Ratio of ductile fracture area (%)		Lateral expansion (mm)	
		Single	Average	Single	Average	Single	Average
CD1	Weld metal	82	85	100	100	1.37	1.41
CD2		83		1.38			
CD3		89		1.49			
CH1	Heat affected zone	177	176	100	100	2.17	2.23
CH2		173		2.20			
CH3		179		2.33			

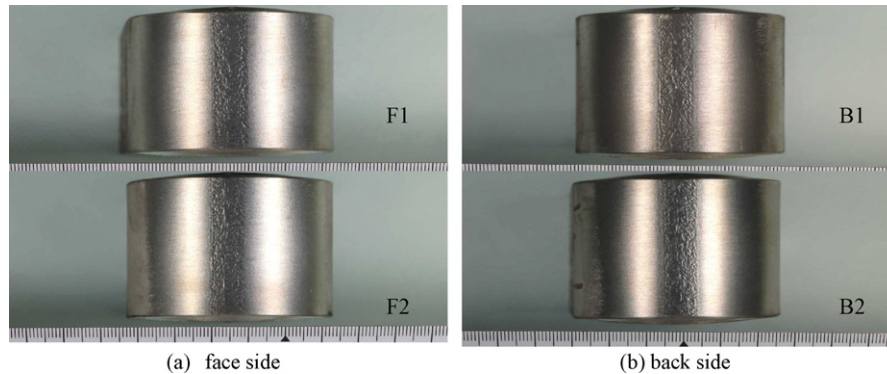


Fig. 9. Photographs of bending test specimens.

4. Conclusions

- (i) When the oxygen concentration in the He-based shielding is in the range of 0.2–2.0%, the weld metal oxygen content is over the critical value of 70 ppm, and an inward Marangoni convection occurs, which makes the weld shape become deep and narrow. When the oxygen content in the shielding gas is below 0.2% or over 2.0%, the Marangoni convection changes from inward to outward and the weld shape become shallow and wide.
- (ii) At the lower welding speed of 0.75 mm/s, the welding current of 160 A and the electrode gap of 1 mm under the He–0.4%O₂ shielding, the weld penetration reaches 9.4 mm for a single pass weld, which is much deeper for Ar–O₂ shielding gas.
- (iii) For He-based shielding gas, a high welding current will strengthen both the inward Marangoni convection on the pool surface and the inward electromagnetic convection in the liquid pool, which make the weld depth/width ratio continuously increase with the welding current.
- (iv) By using the double shielding torch instead of the normal torch for the TIG welding, the degree of the consumption of the tungsten electrode can be same as for normal TIG welding even when an oxidizing gas is included in the shielding gas.
- (v) The joint welded by this new TIG process in which a slightly oxidizing gas is used as the outer gas in the double shielding torch has sound mechanical properties including the tensile, Charpy and bending tests. Therefore, this new double-shielded TIG welding process is definitely applicable for many industrial welding processes.

Acknowledgements

This study was supported by Industrial Technology Research Grant Program from the New Energy and Industrial Technology Development Organization (NEDO) of Japan, the 21st Century and global COE Programs, the ISIJ research promotion grant, and JFE 21st Century Foundation.

References

- [1] S.M. Gurevich, V.N. Zamkov, *Avtom. Svarka*. 12 (1966) 13–16.
- [2] M.M. Savitskii, G.I. Leskov, *Avtom. Svarka*. 9 (1980) 17–22.
- [3] P.J. Modenesi, E.R. Apolimario, I.M. Pereira, *J. Mater. Proc. Technol.* 99 (2000) 260–265.
- [4] S. Kou, Y.H. Wang, *Weld. J.* 65 (1986) 63s–70s.
- [5] D.S. Howse, W. Lucan, *Sci. Technol. Weld. Join.* 5 (2000) 189–193.
- [6] H.C. Ludwig, *Weld. J.* 47 (1968) 234s–240s.
- [7] D. Fan, R.H. Zhang, Y.F. Gu, M. Ushio, *Trans. JWRI* 30 (2001) 35–40.
- [8] S. Sire, S. Marya, *Proceedings of the 7th International Symposium, Kobe, Japan, 2001*, pp. 113–118.
- [9] S. Sire, S. Marya, *Proceedings of the 7th International Symposium, Kobe, Japan, 2001*, pp. 107–112.
- [10] T. Ohji, A. Make, M. Tamura, H. Inoue, K. Nishiguchi, *J. Jpn. Weld. Soc.* 8 (1990) 54–58.
- [11] C.R. Heiple, J.R. Ropper, *Weld. J.* 60 (1981) 143s–145s.
- [12] C.R. Heiple, J.R. Ropper, *Weld. J.* 61 (1982) 97s–102s.
- [13] M. Tanaka, T. Shimizu, H. Terasaki, M. Ushio, F. Koshi-ishi, C.L. Yang, *Sci. Technol. Weld. Join.* 5 (2000) 397–402.
- [14] C.R. Heiple, J.R. Roper, R.T. Stagner, R.J. Aden, *Weld. J.* 62 (1983) 72s–77s.
- [15] H. Fujii, N. Sogabe, M. Kamai, K. Nogi, *Proceedings of the 7th International Symposium, Kobe, Japan, 2001*, pp. 131–136.
- [16] S.P. Lu, H. Fujii, H. Sugiyama, M. Tanaka, K. Nogi, *Mater. Trans.* A43 (2002) 2926–2931.

- [17] S.P. Lu, H. Fujii, H. Sugiyama, K. Nogi, *Metall. Mater. Trans. A34* (2003) 1901–1907.
- [18] J.J. Lowke, M. Tanaka, M. Ushio, *The 57th Annual Assembly of International Institute of Welding, Osaka, Japan, 2004* (IIW Doc.212-1053-04).
- [19] S.P. Lu, H. Fujii, K. Nogi, *Mater. Sci. Eng. A* 380 (2004) 290–297.
- [20] S.P. Lu, H. Fujii, K. Nogi, *Scripta Mater.* 51 (2004) 271–277.
- [21] S.P. Lu, H. Fujii, K. Nogi, *ISIJ Int.* 45 (2005) 66–70.
- [22] K.C. Mills, B.J. Keene, R.F. Brooks, A. Shirali, *Phil. Trans. R. Soc. Lond.* 356A (1988) 911–925.
- [23] P. Sahoo, T. Debroy, M.J. McNallan, *Metall. Trans. B19* (1988) 483–491.
- [24] K. Ishizaki, N. Araki, H. Murai, *Jpn. Weld. Soc.* 34 (1965) 146–153.
- [25] H. Taimatsu, K. Nogi, K. Ogino, *J. High. Temp. Soc.* 18 (1992) 14–19.
- [26] N.S. Tsai, T.W. Eagar, *Metall. Trans. B16* (1985) 841–846.
- [27] M. Tanaka, H. Terasaki, M. Ushio, J.J. Lowke, *The 56th Annual Assembly of International Institute of Welding, Bucharest, Romania, 2003* (IIW Doc.212-1040-03).